ARTICLE NO. 79-0144R

C80-026

Analysis of Weak Glancing Shock/Boundary-Layer Interactions

20003
20015
60001

G.C. Paynter*
Boeing Military Airplane Company, Seattle, Wash.

A flow model is developed for the "weak" glancing shock interaction from experimental observations. Integral continuity, cross-stream momentum, and stream-wise momentum equations are written for a control volume taken about the shock interaction region. Analytic functions are used to represent the 3-D velocity profiles. Given the boundary-layer properties entering the interaction, the integral equations are solved for the boundary-layer properties downstream of the interaction. Computed results are presented for a range of upstream Mach numbers and boundary-layer characteristics over a range of shock strengths. The effects of mass bleed on the interaction are discussed. A comparison between computed results and test data for shock interactions at Mach 2 and Mach 3 indicates the analysis yields the correct trends.

Nomenclature

M = Mach Number
n_{11} = power-law exponent of normal velocity component upstream of the shock interaction
n_{12} = power-law exponent of the normal velocity component downstream of the shock interaction
n_{21} = power-law exponent of the tangential velocity component upstream of shock interaction
n_{22} = power-law exponent of the tangential velocity component downstream of the shock interaction
P = static pressure
$\bar{P}$ = average static pressure on outer surface of control volume
T = static temperature
T_t = total temperature
u = velocity component normal to shock and parallel to surface
V_{CS} = cross stream velocity component
V = magnitude of velocity external to boundary layer
w = velocity component tangential to shock and parallel to surface
y = distance normal to surface
γ = ratio of specific heats
δ = boundary-layer thickness
ϵ = inviscid flow deflection angle
θ = shock angle
ρ = density

Subscripts

1 = upstream of shock
2 = downstream of shock
E,e = local value external to boundary layer

Introduction

ONE technological objective defined at the 1977 NASA Lewis Inlet Workshop[1] was the development of analysis-basis design procedures for 2-D mixed and external compression inlets. The overall Boeing approach to this objective is to extend the existing analysis-based design procedure[2-10] for axisymmetric inlets to 2-D mixed and external compression inlets. This requires identifying flow phenomena present in 2-D inlets which are not present in axisymmetric inlets, the development of a suitable flow analysis for each of these phenomena, the incorporation of these analyses into the design procedure, and the validation of the design procedure over a range of 2-D inlet configurations and flow conditions. The boundary-layer development on the sideplate and the glancing shock/boundary layer interactions on the sideplate were among the flow phenomena identified for which analysis development is required.

Glancing shock/boundary-layer (SBL) interactions occur on the sideplates of 2-D mixed compression or external compression inlets as shown in Fig. 1. These interactions arise when oblique shocks generated by changes in surface slope on the "ramp" or "cowl" surfaces interact with the boundary layer developing on the sideplate. The SBL interaction is three-dimensional since the position of the shock on the sideplate changes in a cross-stream direction; hence the name "glancing" SBL interaction.

Glancing SBL interactions are thought to have an adverse effect on the performance of an inlet. Disturbances originating at the interactions distort the inlet flow field away from that expected from 2-D analysis. Distortion of the inviscid freestream flow generally results in increased total pressure loss. Low momentum boundary-layer flow on the sideplate tends to propagate along the shocks into the corner. This mass flux into the corners increases boundary-layer growth in the corners and distortion of the boundary layers on the ramp and cowl surfaces, resulting in a reduced normal shock stability margin and lower subsonic diffuser total pressure recovery.

Boundary-layer control has been used to reduce the adverse effects of the SBL interactions on inlet performance by removing the low momentum fluid near the wall. (Quantitative data on the effects of boundary-layer bleed on the sideplate boundary-layer development is not available to the author's knowledge.) Sideplate cutback on a 2-D external compression inlet can be viewed as a form of boundary-layer bleed as well.

The purpose of this paper is to present a control volume analysis of weak† glancing SBL interactions suitable for use in an analysis-based inlet design procedure. Discussions of the

Presented as Paper 79-0144 at the 17th Aerospace Sciences Meeting, New Orleans, La., Jan. 15-17, 1979; submitted Jan. 29, 1979; revision received July 23, 1979.

Index categories: Airbreathing Propulsion; Shock Waves and Detonations; Boundary Layers and Convective Heat Transfer—Turbulent.

*Senior Specialist Engineer, Propulsion System Fluid Mechanics Group. Member AIAA.

†Strong interactions are also of interest for inlet design. The flow model used in the analysis of weak interactions presented in this paper is, however, unsuitable for strong interactions.

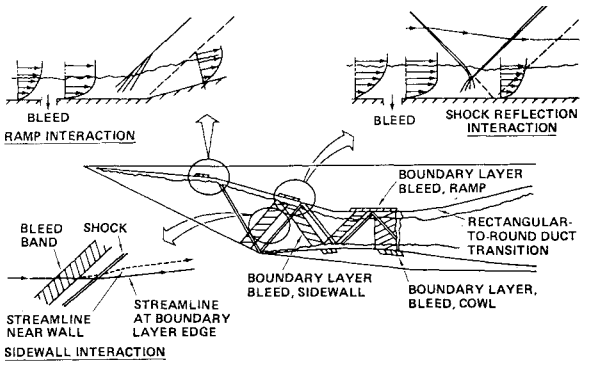

Fig. 1 Two-dimensional inlet flow phenomena.

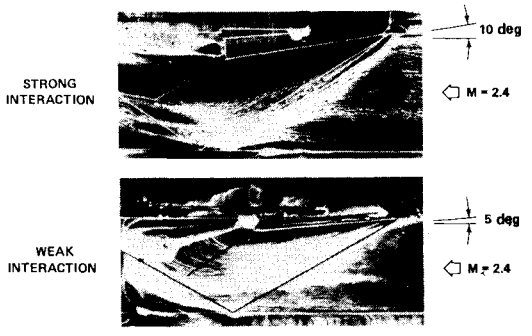

Fig. 2 Wall streamline patterns for weak and strong interactions.

interaction flow phenomena, the flow model, the analysis and solution procedure, comparisons with available data, and the effects of upstream flow properties and boundary-layer bleed on the boundary-layer characteristics downstream of the interaction are presented in the sections which follow.

Flow in the Region of Interaction

Peake[11] defines a weak interaction as one in which there is no coalescence of the streamlines near the wall. Wall streamline patterns for weak and strong interactions are illustrated in Fig. 2 from Dickman.[12] With a fully developed 2-D turbulent boundary layer upstream of the shock interaction, the inviscid static pressure ratio across the shock is $P_2/P_1 \lesssim 1.5$ for a weak interaction.

As noted by Green,[13] the weak interaction resembles a 2-D flow through a normal shock in a plane normal to the shock and the surface. The wall static pressure rise begins 5-10 boundary-layer thicknesses upstream of the inviscid shock location. In this initial interaction region, the wall static pressure rises rapidly and is similar to the "free interaction" pressure rise characteristic of 2-D SBL interactions in a plane normal to the incident shock and the surface.[14] At the incident shock, about half the inviscid static pressure rise has been achieved. For the weak interaction, most of the inviscid pressure rise has been achieved within another 5 boundary-layer thicknesses downstream of the inviscid shock location.

As noted by Oskam et al.,[15] "Freed from the contraint of two-dimensional motion, the fluid can avoid adverse pressure gradients by seeking tangential detours...." Because of the skewing of the incident shock on the sidewall, a strong transverse (normal to the upstream flow direction in a plane parallel to the wall) pressure gradient exists in the region of interaction. This transverse pressure gradient produces a cross flow within the boundary layer in a direction along the shock. Oskam et al.[16] suggest that the process by which cross flows are produced is almost instantaneous in that they occur at the physical location of the pressure gradient. Downstream of the shock, the transverse pressure gradient disappears. The cross flow set up as the boundary layer passes through the region of interaction decays rather slowly as the boundary layer

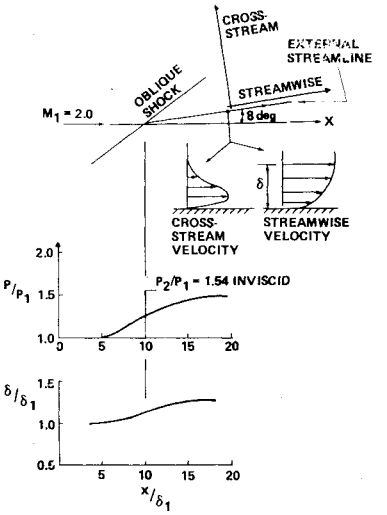

Fig. 3 Shock interaction properties at Mach 2.

develops downstream of the shock. The driving force in the decay process appears to be the magnitude of the cross flow.

The static pressure in the local free-stream flow external to the boundary layer just downstream of the shock is greater than the static pressure on the wall. The difference between the wall static pressure and the local freestream static pressure in this region increases with increasing shock strength. The turning of the flow in this region is somewhat less (~.5 deg) than the shock generator angle. Further from the wall, however, the turning angle and the static pressure rise are about that expected from oblique shock theory. Further downstream of the shock, a rather long (~30δ) region of weak interaction exists in which the boundary-layer cross flow gradually disappears and the wall static pressure gradually rises to the inviscid value.[17]

The boundary layer increases in thickness as it passes through the region of the interaction. The boundary-layer thickness downstream of the interaction is typically larger than that upstream. The wall static pressure and boundary-layer thickness through an interaction at Mach 2 are plotted in Fig. 3 from Peake.[11] Also shown are streamwise and cross-stream velocity distributions downstream of the interaction.

Finally, for a 2-D boundary layer passing through a glancing shock interaction, the flow through the region of interaction is quasi-2-D in a region of sufficient distance from the shock generator.[16] Thus the flow properties in a plane perpendicular to the surface and parallel to the shock are constant or vary slowly with distance along the shock.

Flow Model

The flow model is the set of simplifying assumptions, approximations, and hypotheses used to obtain a solution of the equations of motion for desired but unknown flow characteristics in terms of known flow properties and characteristics. The flow model used to obtain a solution in the current study is based on experimental observations of the flow through the region of interaction and has the following features.

1) The flow is quasi-2-D. The flow properties are assumed constant in a direction parallel to the incident shock. A velocity component in a direction parallel to the shock is assumed to exist.

2) The upstream boundary-layer properties are assumed known.

3) The upstream inviscid flow properties are assumed known.

4) The downstream inviscid flow properties are known from oblique shock theory. As noted in the previous discussion of the interaction flow, this is only approximately

true. Most of the pressure rise occurs in a very localized region near the shock. The local flow external to the boundary layer downstream of the shock is not exactly as computed from oblique shock theory. The flow has turned less than the shock generator angle. The final alignment of the flow and rise in static pressure to the inviscid value occurs over a long region of weak compression downstream of the shock. In the present analysis, this final rise in static pressure and alignment of the local flow external to the boundary layer are assumed to be higher-order effects.

5) The static pressure downstream of the region of the interaction is constant normal to the wall. While the gradient in static pressure normal to the wall in this region increases with increasing shock strength, the experimental data supports this approximation.

6) The region of interaction is "short." This implies that the interaction is essentially inviscid with negligible entrainment and that viscous forces are negligible with respect to pressure forces.

7) The flow in the region of interaction is isoenergetic. This is not an essential assumption and merely avoids solving a separate energy equation for the interaction.

8) The turning of the local inviscid flow external to the boundary layer in a direction away from the wall is supersonic, and the turning of this flow back toward the wall is subsonic for the velocity components in a plane normal to the shock and the wall. This hypothesis is based upon the similarity between the flow through a 2-D normal SBL interaction and the flow in a plane normal to the wall and the shock in the glancing interaction. This hypothesis is used to estimate the pressure force acting on the surface of a control volume about the region of interaction.

9) The velocity components normal and tangential to the shock both upstream and downstream of the region of interaction are well represented as power laws. The use of these very simple velocity profile representations is supported by the available experimental data.

Analysis and Solution Procedure

The flowfield analysis envisioned for the supersonic diffuser portion of a 2-D inlet is as follows. The supersonic inviscid flowfield would be computed with a 2-D "method-of-characteristics" program. The boundary-layer development on ramp and cowl surfaces would be computed with a 2-D boundary-layer analysis. The oblique shocks generated by ramp and cowl surface contours would be located by the inviscid analysis. At intersections between these shocks and the ramp and cowl surfaces, the change in boundary-layer characteristics across the shock would be computed from a control volume analysis, and the 2-D boundary-layer analysis would proceed downstream of a given shock using as initial conditions the boundary-layer properties computed from the control volume analysis. The boundary-layer analysis on the sideplate would be computed in much the same way as that on the ramp and cowl surfaces except that a 3-D boundary-layer analysis would be used. Inviscid flow properties and shock locations on the sideplate would be assumed known from 2-D inviscid analysis. The shock boundary-layer interactions on the sideplate would be treated as discontinuities in the boundary-layer properties. In the context of this overall procedure, the analysis of the glancing SBL interaction flow must provide the change in boundary-layer properties across the interaction. Since the interaction is to be treated as a discontinuity in boundary-layer properties in the overall inlet flow analysis procedure, the detailed flow properties through the region of interaction are not required from the glancing SBL interaction analysis.

A numerical simulation of a strong turbulent glancing SBL interaction has been demonstrated by Hung and MacCormack.[18] The ~1.3 hours of computation time on the CDC 7600 required to compute a single interaction, however, make a Navier-Stokes procedure such as this unsuitable for design. The required computation of perhaps hundreds of glancing SBL interaction cases to achieve a given design forces one to look at much simpler analytical approaches.

A number of factors suggested that a relatively simple analysis could be developed to provide the desired change in boundary-layer properties. These include the following. McCabe[14] developed a simple theory to predict the onset of "incipient separation." This analysis was based on the convection of vorticity through the region of interaction and was successful in predicting the trend of the available data. McCabe's assumption that the boundary-layer flow through the region of interaction is essentially inviscid in nature is supported by the experimental observations of Oskam et al.[16] and Dolling et al.[19] (for strong interactions). Green[13] suggested that the qualitative behavior of the boundary layer through the region of interaction could be obtained by treating the shock interaction as two-dimensional in a plane normal to the shock and the surface, and vectorially adding the upstream velocity component in a direction tangential to the shock. Peake[11] notes that while the flow normal to the shock may appear to be two-dimensional, the density is a scalar quantity and is a function of the cross-stream velocity distribution. The various integral flow properties of the boundary layer will be incorrectly computed unless the effect of the cross-stream velocity component on the density distribution is properly accounted for. Green's suggestion and Peake's comment again point to the relatively simple nature of the interaction flow at least to a first-order level of approximation.

Because of the success of control volume methods for 2-D SBL interactions, as noted by Green[13] and Oates,[20] it seemed natural to try this obvious approach before investigating more complex methods. The short, essentially inviscid, and quasi-2-D nature of the interaction coupled with the success of the McCabe[14] analysis all suggested that a control volume method could be successfully used. The control volume analysis presented herein was intended to demonstrate that this approach is indeed viable.

For the control volume shown in Fig. 4, integral continuity, x-momentum, z-momentum, energy, and state equations may be written as follows:

Continuity:

$$\int_0^{\delta} \rho u \mathrm{d}y \Big|_1 = \int_0^{\delta} \rho u \mathrm{d}y \Big|_2 \tag{1}$$

X-momentum:

$$P_1\delta_1 + \tilde{P}(\delta_2 - \delta_1) - P_2\delta_2 = \int_0^{\delta} \rho u^2 \mathrm{d}y \Big|_2 - \int_0^{\delta} \rho u^2 \mathrm{d}y \Big|_1 \tag{2}$$

Z-momentum:

$$\int_0^{\delta} w\rho u \mathrm{d}y \Big|_1 = \int_0^{\delta} w\rho u \mathrm{d}y \Big|_2 \tag{3}$$

Energy:

$$T_t = \text{constant} \tag{4}$$

State:

$$P = \rho RT \tag{5}$$

With reference to the flow model, note that in the above equations the entrainment and wall shear forces are assumed equal to zero. The boundary-layer velocity profiles upstream and downstream of the region of interaction in directions normal and tangential to the shock are represented as power laws. The boundary-layer thickness is assumed to change through the region of interaction.

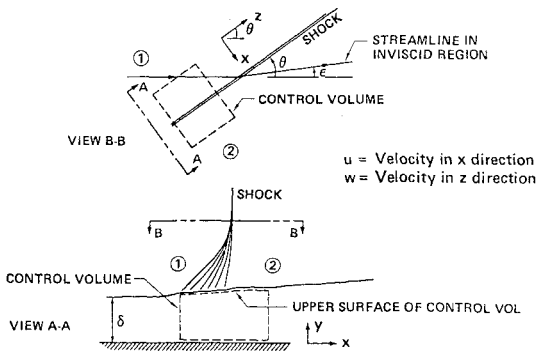

Fig. 4 Control volume.

Normal velocity representation:

$$u/u_e = (y/\delta)^{1/n_{1x}} \tag{6}$$

Tangential velocity representation:

$$w/w_e = (y/r)^{1/n_{2x}} \tag{7}$$

where $x=1$ indicates the profile is upstream of the shock and $x=2$ indicates the profile is downstream of the shock.

The object of the analysis is to obtain the boundary-layer velocity profile parameters δ_2, n_{12}, and n_{22} at state 2 from the known velocity profile parameters at state 1 and the inviscid flow properties upstream and downstream of the incident shock as determined from oblique shock theory. With the auxiliary relationships of Eqs. (4-7), Eqs. (1-3) can be considered three equations for the three unknowns δ_1/δ_2, n_{12}, and n_{22}. Equation 1 can be combined with both Eqs. (2) and (3) to eliminate δ_1/δ_2 as an unknown. Combining Eqs. (1) and (2) yields:

$$\frac{P_2}{P_1}\frac{M_2}{M_1}\left(\frac{1+\left(\frac{\gamma-1}{2}\right)M_2^2}{1+\left(\frac{\gamma-1}{2}\right)M_1^2}\right)^{1/2}\frac{\sin(\theta-\epsilon)\int_0^1\frac{\rho u}{\rho_e u_e}\mathrm{d}(y/\delta)\Big|_2}{\sin(\theta)\int_0^1\frac{\rho u}{\rho_e u_e}\mathrm{d}(y/\delta)\Big|_1}$$

$$-\frac{\left[\frac{P_2}{P_1}-\frac{\bar{P}}{P_1}+\frac{P_2}{P_1}\gamma M_2^2\sin^2(\theta-\epsilon)\int_0^1\frac{\rho u^2}{\rho_e u^2{}_e}\mathrm{d}(y/\delta)\Big|_2\right]}{\left[1-\frac{\bar{P}}{P_1}+\gamma M_1^2\sin^2\theta\int_0^1\frac{\rho u^2}{\rho_e u^2{}_e}\mathrm{d}(y/\delta)\Big|_1\right]}=0$$

$$=F(n_{12},n_{22}) \tag{8}$$

Combining Eqs. (1) and (3) yields:

$$\left(\frac{1+\left(\frac{\gamma-1}{2}\right)M_2^2}{1+\left(\frac{\gamma-1}{2}\right)M_1^2}\right)^{1/2}\frac{\int_0^1\frac{\rho u}{\rho_e u_e}\mathrm{d}(y/\delta)\Big|_2}{\int_0^1\frac{\rho u}{\rho_e u_e}\mathrm{d}(y/\delta)\Big|_1}$$

$$-\left\{\frac{M_2}{M_1}\frac{\cos(\theta-\epsilon)}{\cos\theta}\frac{\int_0^1\frac{\rho u w}{\rho_e u_e w_e}\mathrm{d}(y/\delta)\Big|_2}{\int_0^1\frac{\rho u w}{\rho_e u_e w_e}\mathrm{d}(y/\delta)\Big|_1}\right\}=0=G(n_{12},n_{22}) \tag{9}$$

Note that the term $\bar{P}$ which appears in Eq. 8 is the average pressure acting on the upper surface of the control volume. If one assumes that the turning away from the wall is supersonic

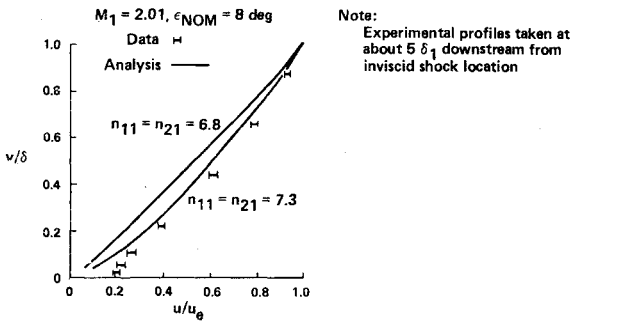

Fig. 5 Computed and measured velocity profiles normal to the shock.

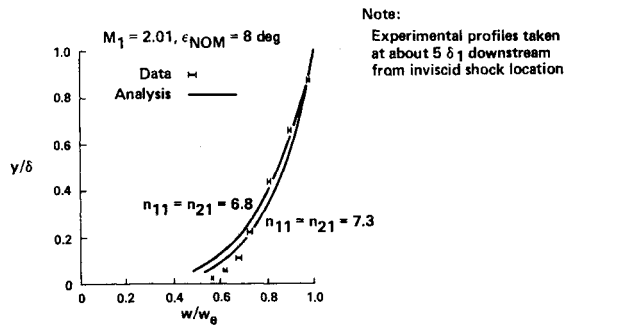

Fig. 6 Computed and measured velocity profiles tangential to the shock.

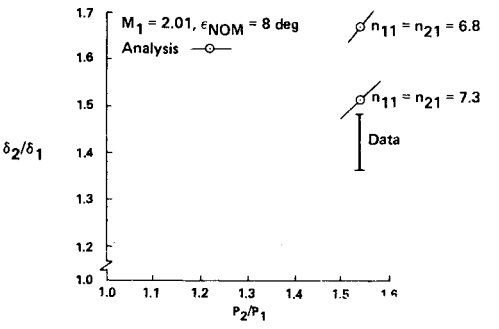

Fig. 7 Computed and measured change in δ across the interaction.

and the turning back toward the wall is subsonic in terms of the velocity components in a plane normal to the shock and the wall, one can show that $\bar{P}/P_1$ can be approximated by the expression,

$$\frac{\bar{P}}{P_1}=.67\frac{P_2}{P_1}+.33\left\{\frac{[1.+[(\gamma-1)/2]M_1^2\sin^2\theta]}{1+[(\gamma-1)/2]}\right\}^{\gamma/(\gamma-1)} \tag{10}$$

With Eq. (10) substituted for $\bar{P}/P_1$ in Eq. (8), Eqs. (8) and (9) now form a system of two equations for the two unknowns n_{12} and n_{22}. Equations (8) and (9) are solved iteratively with a Newton-Raphson scheme. The integrals appearing in the equations are evaluated with a numerical integration procedure. δ_1/δ_2 is obtained from Eq. (1). Typical run times for a case are 0.3-0.5 CPU s on the Cyber 175 computer.

Comparisons of Experimental and Predicted Results

Results of the calculation procedure are compared with experimenal data by Peake[11] in Fig. 5-7 for an interaction flow at $M_1=2.01$ and a nominal deflection angle of 8 deg. The nominal static pressure rise across the interaction was 1.54 and $Re_{\delta 1}\cong 1.5\times 10^5$. The boundary layer upstream of the interaction was two-dimensional with a power-law exponent between 6.8 and 7.3. The upstream power-law ex-

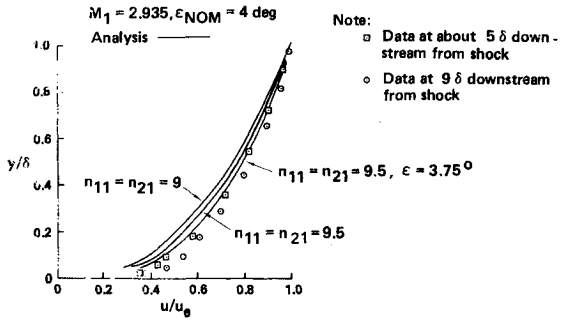

Fig. 8 Computed and measured velocity profiles normal to the shock.

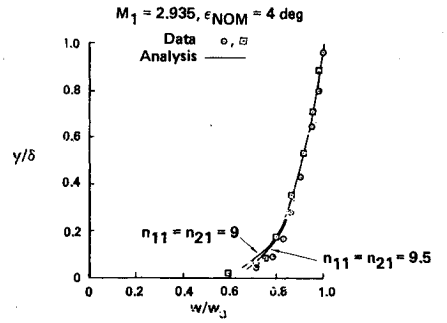

Fig. 9 Computed and measured velocity profiles tangential to the shock.

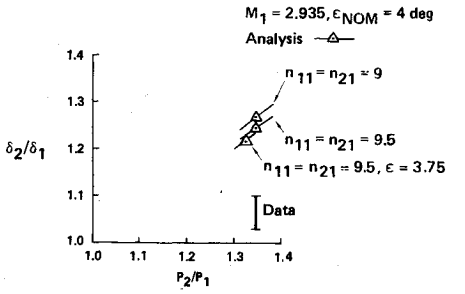

Fig. 10 Computed and measured change in δ across the interaction.

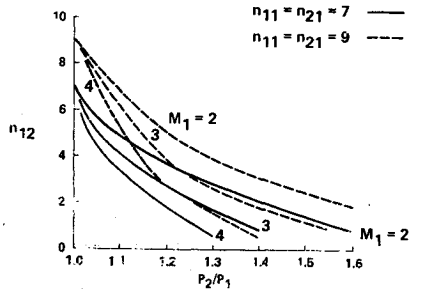

Fig. 11 Profile exponent of normal velocity component.

ponent and the boundary-layer thickness both upstream and downstream of the interaction were determined by fitting a straight line through a log-log plot of u/u_e vs y/δ where δ is defined as the y value at which the straight-line fit through the velocity data intersects the line $u/u_e = 1$. The local velocity was computed by Peake from an assumption that the local static pressure was uniform through the boundary layer and equal to the wall value at a given station on the sidewall. It is also worth noting that in this experiment the shock generator was translated axially to move the shock interaction axially relative to fixed probe traverse stations. The wall temperature was approximately equal to the adiabatic wall value through the interaction.

The predicted velocity component profile downstream of and normal to the shock is compared with test data in Fig. 5. The predicted velocity profile component downstream of and tangential to the shock is compared with test data in Fig. 6. The predicted change in boundary-layer thickness across the interaction is given in Fig. 7. The analysis somewhat over-predicts the distortion of the normal and tangential velocity components and the change in boundary-layer thickness across the interaction.

Results of the calculation are compared with experimental data by Oskam[21] et al. in Figs. 8-10 for an interaction flow at $M_I = 2.935$ and a nominal deflection angle of 4 deg. The nominal static pressure rise across the interaction was 1.344 and $Re_{\delta I} \simeq 8 \times 10^5$. The boundary layer upstream of the interaction was the tunnel wall boundary layer with a power-law exponent of between 9.0 and 9.5. The power-law exponents of the boundary layer upstream and downstream of the interaction were determined as described above for the Peake data. Velocity components were computed from total temperature, total pressure, static pressure, and yaw angle measurements taken at several fixed traverse stations both upstream and downstream of the shock interaction. The stagnation temperature of the tunnel was not controlled and varied somewhat during the course of a run and from day to day. These effects are believed to be insignificant, and the tunnel wall boundary layer was assumed to be at about the adiabatic wall temperature.

The predicted velocity component downstream of and normal to the shock is compared with test data in Fig. 8. The predicted velocity component downstream of and tangential to the shock is compared with test data in Fig. 9. The predicted change in the boundary-layer thickness across the interaction is given in Fig. 10. As for the Peake data, the analysis somewhat over-predicts the distortion of the normal and tangential velocity components. The analysis also over-predicts the change in boundary-layer thickness across the interaction. The difference between computed and measured change in boundary-layer thickness is somewhat greater than expected. This may be due to a transverse nonuniformity of the tunnel wall boundary layer entering the interaction in the Oskam et al. experiment. The boundary-layer velocity profile data upstream of the shock were taken near the center of the wind-tunnel sideplate used for the study. The boundary-layer velocity profile data downstream of the shock were taken closer to the side of the test section. A transverse nonuniformity of the boundary layer on the sideplate could explain the lack of agreement for the change in thickness across the region of interaction.

The analysis clearly predicts the correct trend for the distortion of the downstream velocity profile components and the correct trend for the change in boundary-layer thickness across the interaction. The power-law velocity profile representations for the velocity components normal and tangential to the shock appear to be adequate. A law-of-the-wall law-of-the-wake representation could perhaps be developed that would yield better agreement in the region close to the wall. The over-prediction of the component velocity profile distortion and the change in boundary-layer thickness are as expected from the assumptions made in the flow model. In the flow model, the full rise in static pressure is assumed to occur at the interaction. In the actual flow, while most of the static pressure rise occurs locally near the shock, the final rise to the inviscid value is associated with a long region of boundary-layer redevelopment downstream of the shock. The present flow model "decouples" the boundary-layer redevelopment from the static pressure rise. Thus the computed distortion of the boundary layer immediately downstream of the shock will be somewhat greater than one would observe for the actual flow.

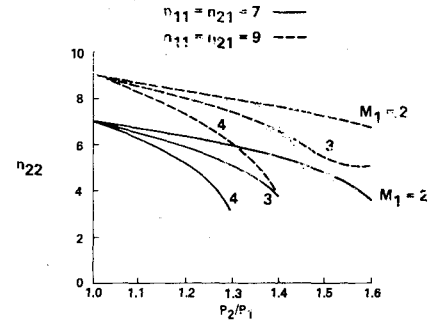

Fig. 12 Profile exponent of tangential velocity component.

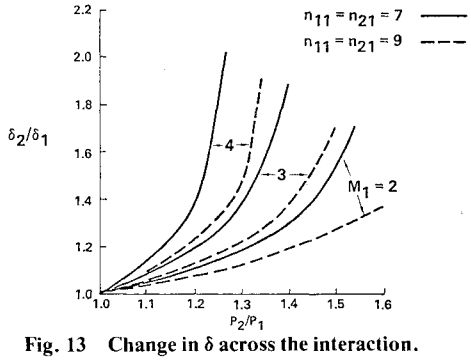

Fig. 13 Change in δ across the interaction.

Results for a Parametric Variation of Initial Conditions

The predicted effects of shock strength, Mach number, and upstream boundary-layer profile shape on the power-law exponent of the normal velocity component profile are shown in Fig. 11. Upstream velocity profile exponents of 7 and 9 and upstream Mach numbers of 2, 3, and 4 were considered. At a given upstream Mach number, a decrease in n_{12} with an increase in shock strength is predicted. At a given Mach number and shock strength, an increase in the upstream profile exponent results in an increase in n_{12}.

The predicted effects of shock strength, Mach number, and upstream profile shape on the power-law exponent of the tangential velocity component profile are shown in Fig. 12 for the same range of upstream Mach numbers, profile exponents, and shock strengths as Fig. 11. The predicted trends of n_{22} with shock strength, upstream Mach number, and velocity profile exponent are the same as for n_{12}. At a given shock strength, etc., $n_{22} > n_{12}$.

The predicted effects of shock strength, upstream profile shape, and Mach number on the ratio of downstream to upstream boundary-layer thickness δ_2/δ_1 are shown in Fig. 13. At a given Mach number, the predicted δ_2/δ_1 increases with increasing shock strength. At a given Mach number and shock strength, raising the upstream power-law exponent reduces δ_2/δ_1.

Boundary-layer bleed on the sideplate of a 2-D inlet could be used to control the development of the boundary layer through the interaction. Bleed holes would typically be located in a band upstream of and parallel to the shock so that at off-design operating conditions, the shock would travel forward toward the bleed band. The effect of this upstream bleed on the boundary layer entering the shock interaction would be to reduce the thickness of the boundary layer and increase the "fullness" of the velocity profile. Increasing the "fullness" of the velocity profile is equivalent to raising the power-law exponent of the boundary layer. At a given upstream Mach number and shock strength, bleed would thus reduce δ_2/δ_1 and increase the "fullness" of the component velocity profiles normal and tangential to the shock. These effects were illustrated in Figs. 11, 12, and 13. The effects of

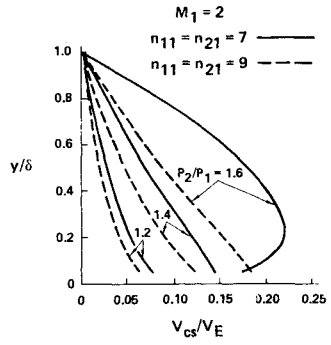

Fig. 14 Cross flow as a function of shock strength.

upstream bleed on the cross-flow downstream of the shock interaction are illustrated in Fig. 14 for three shock interactions at $M_1 = 2$. These cross-flow profiles were computed from the predicted normal and tangential velocity profiles. As one might expect, boundary-layer bleed which acts to increase the upstream power-law exponent results in a reduced cross-flow.

Many other bleed configurations are possible and may perhaps offer advantages relative to the type of system described above. Bogdonoff[22] has suggested, for example, allowing the cross-flow along the shock to develop and using boundary-layer bleed in the corners to control the adverse effects associated with these interactions. Each scheme would have to be evaluated for a given airplane and mission. The above comments as to the effects of bleed on the interaction are intended to illustrate the effects of a typical bleed system on the interaction.

Conclusions

A control volume analysis was developed to predict the change in integral boundary-layer properties across a weak glancing shock/boundary-layer interaction. Comparisons between computed results and test data for interactions at Mach 2 and 3 indicate that the analysis yields the correct trends. These results demonstrate the viability of this analytical approach to achieve a computer-efficient component analysis suitable for use in an overall inlet flow analysis useful for design.

Computed results are presented to illustrate the effects of upstream Mach number, upstream boundary-layer characteristics, and shock strength on the boundary-layer characteristics downstream of the interaction. The analysis indicates that upstream boundary-layer bleed would reduce the change in boundary-layer thickness across the interaction and result in less cross-flow downstream of the interaction.

Further experimental work on weak glancing SBL interactions is desirable. The validity of the analysis should be evaluated over a much broader range of shock strengths, upstream Mach numbers, and upstream boundary-layer properties than was possible in the present study due to the lack of suitable data. The effects of bleed on the interaction should be investigated experimentally. The analysis could easily be extended to include the effects of non-adiabatic wall conditions, variable γ, and bleed and to improve the velocity profile representations and pressure interaction modeling. To validate these potential improvements, suitable data must be obtained from experiments structured to provide the necessary detailed flow properties. The results of Navier-Stokes procedures could be explored for use as "numerical experiments" to further validate the analysis and possible improvements to the analysis.

References

[1] *Proceedings of the 1977 NASA Lewis Inlet Workshop.*

[2] Koncsek, J.L. and Syberg, J., "Transonic and Supersonic Test of

a Mach 2.65 Mixed-Compression Axisymmetric Intake," NASA CR-1977, March 1972.

[3] Syberg, J. and Koncsek, J.L., "SST Technology Follow-On Program, Phase I, Transonic and Supersonic Test of the SST Prototype Air Intake," The Boeing Company, Rept. no. FAA-SS-72-50, April 1972.

[4] Reyhner, T.A. and Hickcox, T.E., "A Procedure for Combined Viscous-Inviscid Analysis of Supersonic Inlet Flowfields," *Journal of Aircraft,* Vol. 9, Aug. 1972, pp. 589-595.

[5] Syberg, J. and Koncsek, J.L., "Bleed System Design Technology for Supersonic Inlets," *Journal of Aircraft,* Volume 10, July 1973, pp. 407-413.

[6] Syberg, J. and Hickcox, T.E., "Design of a Bleed System for a Mach 3.5 Inlet," NASA CR-2187, Jan. 1973.

[7] Syberg, J. and Koncsek, J.L., "Experimental Evaluation of a Mach 3.5 Axisymmetric Inlet," NASA CR-2563, July 1975.

[8] Syberg, J. and Hickcox, T.E., "(Title Secret)," Boeing Document D6-42992, May 1976. (Prepared under subcontract S10-3304 for Lockheed—California Company).

[9] Syberg, J. and Hickcox, T.E., "Interactive Bleed System Design for High Speed Inlets," presented at the NASA-Lewis Inlet Workshop, Jan. 11-13, 1977.

[10] Syberg, J., "Analytic Design of AST Inlet," Boeing Document D180-20551-1, March 1977.

[11] Peake, D.J., "Three-Dimensional Swept Shock/Turbulent Boundary-Layer Separations With Control By Air Injection," National Research Council Canada, Aero. Report LR-592, July 1976.

[12] Dickman, C.C., "Glancing Interaction With a Turbulent Boundary Layer," AFOSR-76-3006 July 1977.

[13] Green, J.E., "Interactions Between Shock Waves and Turbulent Boundary Layers," *Progress In Aerospace Sciences,* Vol. 11, Pergamon Press, Oxford, 1970, pp. 235-340.

[14] McCabe, A., "The Three-Dimensional Interaction of a Shock Wave With a Turbulent Boundary Layer," *Aeronautical Quarterly,* Aug. 1966, pp. 231-252.

[15] Oskam, B., Vas, I.E., and Bogdonoff, S.M., "Mach 3.0 Oblique Shock Wave/Turbulent Boundary-Layer Interactions in Three Dimensions," AIAA Paper 76-336, 9th Fluid and Plasma Dynamics Conf., San Diego, Calif., July 14-16, 1976.

[16] Oskam, B., Vas, I.E., and Bogdonoff, S.M., "An Exploratory Study of a Three-Dimensional Shock Wave Boundary-Layer Interaction at Mach 3," Princeton University, Rept. 1227, May 1975.

[17] Neumann, R.I. and Token, K.H., "Prediction of Surface Phenomena Induced by Three-Dimensional Interactions on Planar Turbulent Boundary Layers," International Astronautical Federation XXV Congress, Paper No. 74-058, Amsterdam, Oct. 1974.

[18] Hung, C.M. and MacCormack, R.W., "Numerical Solution of Three-Dimensional Shock Wave and Turbulent Boundary-Layer Interaction," AIAA Paper 78-161, 16th Aerospace Sciences Meeting, Huntsville, Ala., Jan. 1978.

[19] Dolling, D.S., Cosod, C.D., and Bogdonoff, S.M., "Three-Dimensional Shock Wave Boundary-Layer Interactions—A Parametric Study of Blunt Fin-Induced Flows," AIAA Paper 78-159, 16th Aerospace Sciences Meeting, Huntsville, Ala., Jan. 1978.

[20] Oates, G.C., "Lecture Notes on Shock Boundary-Layer Interaction," VKI Lecture Series No. 86, March 1976.

[21] Oskam, B., Vas, I.E., and Bogdonoff, S.M., "Oblique Shock Wave/Turbulent Boundary-Layer Interactions In Three Dimensions at Mach 3—Part II," AFFDL TR-76-48, Part II, March 1978.

[22] Bogdonoff, S.M., private communication, Sept. 1978.